DOI: https://doi.org/10.31351/vol35iss1pp98-111

Molecular Docking, ADMET Study, Synthesis, Characterization, and Anti-proliferative Activity Study of Novel Schiff Base Derivatives of N'-benzylidene-4H-benzo[b][1,4]thiazine-3-carbohydrazide Against Lung Cancer Cell Line.

Haider J. Al-Karagully*,[1] and Mohammed Kamil Hadi[2]

[1]Ministry of Health, The National Center of Drug Control and Research (NCDCR), Baghdad, Iraq.
[2]Department of Pharmaceutical Chemistry, College of Pharmacy, University of Baghdad, Bagdad, Iraq.
***Corresponding author**

Received 23/11/2025, Accepted 20/2/2025, Published 29/3/2026

This work is licensed under a Creative Commons Attribution 4.0 International License.

Abstract

Epidermal growth factor receptor tyrosine kinase (EGFR-TK) is a vastly fascinating epigenetic target for medicine treatment. EGFR-TK is overexpressed in several diseases, including cancers. In this study, we designed new EGFR-TK inhibitors with the same consists of erlotinib (approved anticancer drug) with longer linker and substituted hydrophobic moiety using Ligand Designer from Glide (Schrodinger LLC). By experimenting with different amide and Schiff base residues, the linker was optimized. Using licensed Schrodinger modeling software, the probable inhibition over EGFR-TK for the best-designed items was virtually assessed. The findings demonstrated that there is a possibility of an acceptable level of fitness interaction between the hydroxylated substitution hydrophobic moiety and the EGFR-TK active site. To forecast the final drugs' pharmacokinetic characteristics, an ADMET analysis was conducted. Good predicted drug-like characteristics were displayed by the final compounds. Recrystallization was used to successfully manufacture and purify the intermediates and final compounds. FTIR, ^{1}HNMR, and ^{13}CNMR spectroscopic analysis were used to characterize the chemical structure of the intermediates and final products. Using the MTT assay; all synthesized compounds (SH1-SH6) exposed a reassuring antiproliferative activity in A504 lung tumor cell lines with low IC50, and good inhibition percentage comparable to the reference standard of erlotinib. The compound SH6 was the most promising one which has an IC50=3.88µM and a percentage of inhibition=94.1%, compared with erlotinib, a reference authorized anticancer drug which has an IC50 of 3.86 µM and an inhibition percentage of 94.7%.

Keywords: ADMET, Benzothiazine, Erlotinib, Lung Cancer, Molecular Docking, Schiff Base.

Introduction

One of the most common causes of disease and mortality nowadays is the malignant development of different tissues. The World Health Organization's data rank colon, rectal, breast, lung, and prostate cancers highest among other malignancies [(1)].

Cancer is one of the major global health burdens representing the second major cause of death worldwide (WHO 2020) [(2)].

Globally, there is a lot of focus on the discovery and development of anticancer medications. There are currently numerous substances in use, each with a unique antiproliferative mechanism of action. Alkylating agents, antimetabolites, cytotoxic antibiotics, alkaloids, plant medicines, and other categories are generally used to categorize antineoplastics. complexing compounds from platinum cytostatic, protein kinase inhibitors, and monoclonal antibodies [(3-7)].

Compounds with potential efficacy that have higher pharmacodynamic and kinetic qualities and lower toxicity are still in high demand as therapeutic agents [(8)]. Different medications work well for different kinds of tumor growth. It can be said that one of the main issues that combination therapy attempts to solve is the resilience of tumor cells. Professionals and the general public are currently concentrating on the therapeutic application of nanoparticles and nano-formulated antineoplastics as well as a variety of drug-delivery nano-systems [(9-10)].

Combining heterocycles offers a new opportunity to create novel multicyclic compounds with improved biological activity [(11)].

Cell integrity and bodily balance depend on apoptosis, which is a type of controlled, self-automated cell death. Moreover, a number of illnesses, including breast cancer, can develop as a result of poor apoptotic process execution. [12] Therefore, one promising approach to treating hormone-sensitive breast cancer is to target the regulators or inducers of apoptosis in cancer cells. The apoptogenic theory states that apoptotic signaling pathways can be induced and stimulated by aromatase inhibition, which suppresses estrogen production and lowers the risk of hormone-dependent breast cancer growth [13].

Heterocyclic compounds interact with a broad range of biological targets because of their structures [14–16], and they are definitely crucial in the development of antineoplastics [17-19].

The primary feature of protease inhibitors that may be prescribed for their anti-proliferative agent applications is their capacity to increase the susceptibility of cancer cells to chemotherapy and radiation [20].

In medicinal chemistry, the chief goal is to synthesize promising activity compounds acting as therapeutic agents with lower side effects [21].

Sulfur and nitrogen-containing scaffold, 1,4-benzothiazine (1,4-B), has attracted continuing interest and has become an important construction motif for developing new drug candidates [22]. The name 1,4-benzothiazine is applied to both 2H- and 4H-isomer of the molecule where 4H-1,4-benzothiazine analogs have been extensively studied for decades [23]. One of the most valuable structural features of 4H-1,4 benzothiazine to impart a diverse range of activity is the occurrence of the fold along the nitrogen and sulfur axis [24]. The compounds containing 4H-1,4 skeleton possess significant anticancer activity and many other pharmacological activities such as central nervous system activity, anti-inflammatory, cardiovascular, and antimicrobial [25-27].

While, Schiff bases have been widely studied and are the focus of different research, due to their extensive use and distinct pharmacological activities [28].

Tumor is one of the most prevalent diseases in the world. As the leading cause of cancer-related mortality, lung cancer is one of the most common cancers, accounting for almost 1.7 million cancer-related deaths worldwide in 2018 alone [29]. From a histological perspective, lung cancer can be classified into two types: small-cell lung cancer (SCLC) and non-small-cell lung cancer (NSCLC). NSCLC is the cause of approximately 85% of all lung malignancies worldwide, including adenocarcinoma, squamous-cell carcinoma, and large-cell carcinoma [30–31]. Even now, lung cancer is a fatal illness. Nonetheless, a number of advancements, including better diagnosis and the creation of novel medications, have resulted in a sharp increase in the five-year survival rate [32–33]. This article was regarding the synthesis of novel derivatives containing 1,4-benzothiazine scaffolds with predicted anti-proliferative activity. optimization of protein structures) was generated. The Schrodinger program 13.1 (1–2023) was used to optimize H-bond assignments with default settings and clean up the structure using the OPLS (2005) force field (Orthogonal Partial Least Squares (OPLS) enables to separately model the variation correlated (predictive) to the factor of interest and the uncorrelated (orthogonal) variation. While performing similarly to PLS, OPLS facilitates interpretation). Using the default configuration, which limited the grid size to 15A*15A*15A, the co-crystallized ligand that interacted with the protein was used to create the receptor grid. The set of ligands to be docked is identified and prepared using ligprep, which incorporates tautomeric, stereochemical, and ionization states in addition to energy minimization using the OPLS (2005) force field. This approach goes beyond straightforward 2D and 3D structure conversion. Using the default SP docking configuration, which limits out to 10 poses, the produced ligands were docked with EGFR (4HJO). The ligand's fitness in the active site was used to visualize the resulting poses [35].

Materials and Methods

Molecular Docking

The Glide application, which is integrated with the maestro software from the licensed Schrodinger's modeling suite version 13.0135, was used to conduct docking research, to create a novel Epidermal Growth Factor Receptor Tyrosine Kinase (EGFR_TK), Ligand Designer produced virtual molecules. The hydrophobic core, linker, terminal hydrophobic moiety, and terminal substitution of the proposed derivatives resembled the general pharmacophoric characteristics of erlotinib. With erlotinib as a co-crystallized ligand, the protein was selected from the HOMO sapiens to mimic a substance that would be effective on people. A protein data library provides the EGFR-TK (4HJO) crystal structure [34]. As part of the protein preparation wizard, the protein was preprocessed to allocate bond order, hydrogen was added, terminal oxygen was added to the chain, water beyond 3 A^0 was removed from the ligand, water beyond 3 A^o from the ligand formed less than 3 hydrogen bonds with the ligand or amino acid had less chance of affecting the docking, from the active site, and het stat with EPiK (a software tool developed by Schrödinger for the preparation and

ADMET studies

To evaluate the drug-likeness of the suggested compounds, the produced ligands are subjected to ligand-base ADMET prediction. The software was configured by QIKProp to find the five most similar drug molecules, and the output data was examined to determine the developed compounds' drug potential.

Chemical synthesis

Materials

The chemicals and solvents were purchased from different suppliers such as Sigma-Aldrich, Loba Chimei (India), hyper-chem (China), and Scharlau (Spain). Fine, were put to use without being further cleaned. Using a 20*20 cm TLC silica gel 60 F254 sheet from Merck KGaA, thin-layer chromatography (TLC) was carried out and detected at 254 nm UV light. The Shimadzu IRAffinity-1 Spectrometer (Shimadzu, Japan) was used to perform FT IR spectroscopy at the University of Baghdad's College of Pharmacy's Pharmaceutical Chemistry department. The Mansoura University-Faculty of Pharmacy conducted ^{1}HNMR analyses at 400 MHz and ^{13}C-NMR at 100 MHz (with d6-DMSO as the solvent) utilizing a Bruker Avance III.

General procedure for the synthesis of ethyl 4H-benzo[b][1,4]thiazine-3-carboxylate (compound A) (36-37)

A mixture of 2-amino-thiophenol (0.01 mol/ 1.25g) and ethyl bromopyruvate (0.01 mol/ 1.95g) in absolute ethanol 50ml with constant stirring in RBF for 18 h (at room temperature), and then it was stood aside to cool; the precipitate was filtered by using ash-free filter paper, wash and purified by recrystallization from ethyl alcohol to yield (78%) a yellow powder. I.R: 3047, 2978, 2935, 2900, 1708, 1608, 1577, 1442, 1226, 1087 and 780 cm^{-1}. ^{1}HNMR (400 MHz, DMSO) δ 7.71 – 7.62 (m, 3H, Ar-CH), 7.49– 7.34 (m, 3H, Ar-CH), 4.24 – 4.12 (m, 2H, CH2), 1.22 (t, 3H, CH3). ^{13}CNMR: δ 161, 149, 133, 131, 128, 126, 123, 117, 115, 62.66 and 13.98

General procedure for synthesis of 4H-benzo[b][1,4]thiazine-3-carbohydrazide (compound B) (38-39)

A solution of 0.01 mol/ 2.21g of (compound A) in 30 mL of absolute methanol, hydrazine hydrate (0.1 mol, 80%/ 5g) was added step by step in a 100 ml RBF, followed by a catalytic amount of conc. H_2SO_4 (10 drops/ 0.5 ml). The reaction mixture was refluxed for 8 h. The solid powder separated and excess solvent was removed by a rotary evaporator. The residue was recrystallized from methanol and the product dried to yield (82%) an orange crystalline powder. I.R: 3387, 3340, 3286, 3248, 3197, 3159, 2904, 1670, 1612, 1581, 1500, 1473, 1396, 1053 and 741 cm^{-1}. ^{1}HNMR (400 MHz, DMSO) δ 9.35 (s, 1H, Acyc-NH), 7.59 (s, 1H, Ar-CH), 7.03 – 6.95 (m, 2H, Ar-CH), 6.91 – 6.84 (m, 2H, Ar-CH), 6.74 (s, 1H, Cyc-NH), 4.38 (d, J = 3.9 Hz, 2H, NH2). ^{13}CNMR: δ 167, 156, 131, 129, 128, 126, 123, 118 and 115.

General procedure for the synthesis of hydrazide derivatives as Schiff bases (SH1–SH6) (40-41)

An equimolar of compound (B) and substituted aldehydes was taken in 100 ml RBF with methanol 25 ml and refluxed for 18 h. in the presence of 10 ml orthophosphoric acid (2-5) drops. TLC monitored the reaction until the precipitate appeared. The precipitate was collected by removing the excess solvent and then filtration using an ash-free filter paper, recrystallized by methanol to give a finished product (SH1-SH6).

Compound **SH1((E)-N'-benzylidene-4H-benzo[b][1,4]thiazine-3-carbohydrazide)** yield is (87%) as a pink color powder; I.R: 3379, 3325, 3267, 3251, 3051, 3024, 2360, 2337, 1637, 1581, 1523, 1477, 1431, 1315 and 736 cm^{-1}. ^{1}HNMR (400 MHz, DMSO) δ 11.76 (s, 1H, Acyc-NH), 8.39 (s, 1H, Acyc-CH), 7.85 – 7.79 (m, 3H, Ar-CH), 7.77 – 7.64 (m, 4H, Ar-CH), 6.93 – 6.87 (m, 3H, Ar CH), 6.78 (s, 1H, Cyc-NH). ^{13}CNMR: δ 163, 151, 142, 130, 129 (for two symmetrical carbons), 128 (for two symmetrical carbons), 127.8, 127.6, 123, 119, 116, and 114.8

Compound **SH2 (N'-((1E,2E)-3-phenylallylidene)-4H-benzo[b][1,4]thiazine-3-carbohydrazide)** yield is (82%) as a dark red powder; I.R: 3637, 3367, 3298, 3047, 2927, 1658, 1624, 1581, 1473, 1427, 1323, 1184, 1184, 979 and 740 cm^{-1}. ^{1}HNMR (400 MHz, DMSO) δ 11.52 (s, 1H, Acyc-NH), 7.73 7.64 (m, 1H, Ar-CH), 7.63 (s, 1H, Ar-CH), 7.49 (s, 1H, Ar CH), 7.40 – 7.33 (m, 5H, Ar-CH), 7.15 – 7.07 (m, 2H, Ar-CH), 6.99 – 6.94 (m, 3H, Acyc-CH), 6.80 (s, 1H, Cyc-NH). ^{13}CNMR: δ 164, 151, 136, 135, 130, 129.5 (for two symmetrical carbons), 129.4, 129.3, 128 (for two symmetrical carbons), 127.8, 127.6, 125.7, 125.3, 123, 119 and 114.8.

Compound SH3 **((E)-N'-(4-methoxybenzylidene)-4H-benzo[b][1,4]thiazine-3-carbohydrazide)** yield is (86%) as a red powder; I.R: 3332, 3228, 3047, 2931, 2908, 2835, 1666, 1631, 1600, 1508, 1465, 1307, 1253, 1168,1029, 833 and 744 cm^{-1}. ^{1}HNMR (400 MHz, DMSO) δ 11.59(s, 1H, Acyc NH) 8.31 (s, 1H, Acyc-CH), 7.83 – 7.73 (m, 2H, Ar CH), 7.70 – 7.63 (m, 1H, Ar-CH), 7.55 (s, 1H, Ar CH), 7.06 – 6.96 (m, 3H, Ar-CH), 6.92(m, 3H, Ar CH), 6.78 (s, 1H, Cyc-NH), 3.80 (s, 3H, CH3). ^{13}CNMR: δ 164, 159, 149, 141, 139, 131,130, 129, 128, 127, 126.5, 126.7, 123,119, 114.87, 114.83, and 114.5.

Compound **SH4 ((E)-N'-(4-hydroxybenzylidene)-4H-benzo[b][1,4]thiazine-3-carbohydrazide**) yield is (78%) as a dark yellow powder; I.R: 3332,3217, 1651, 1600, 1581,1512,

1431, 1165, and 744cm^{-1}. ^{1}HNMR (400 MHz, DMSO) δ 11.48 (s, 1H, Acyc-NH), 10.04 (s, 1H, OH), 8.25 (s, 1H, Acyc-CH), 7.76 (s, 1H, Ar-CH), 7.67– 7.61 (m, 2H, Ar-CH), 7.53 (s, 1H, Ar-CH), 7.01 (m, 1H, Ar CH), 6.94 (m, 3H, Ar-CH), 6.73 (s, 1H, Cyc-NH). ^{13}CNMR: δ 163, 157, 149, 141, 131, 130, 129, 128, 126.7, 126.4, 125, 123, 119, 116.5, and 116.2.

Compound **SH5 ((E)-N'-(2-hydroxybenzylidene)-4H-benzo[b][1,4]thiazine-3-carbohydrazide)** yield is (88%) as a brown powder; I.R: 3352, 3051, 1681, 1631, 1620, 1585, 1473, 1311, 1269, 1149 and 740cm^{-1}. ^{1}HNMR (400 MHz, DMSO) δ 12.00 (s, 1H, OH), 10.86 (s, 1H, Ar-NH), 8.63 (s, 1H, Acyc-), 7.70 – 7.63 (m, 1HAr-CH), 7.32 (s, 1H, Ar-CH), 7.13 – 7.02 (m, 1H, Ar-CH), 6.95 (m, 4H, Ar-CH), 6.83 – 6.74 (m, 2H, Ar-CH), 6.67 (s, 1H, Cyc-NH). ^{13}CNMR: δ 165, 157, 148, 141, 133, 132, 130, 129, 128, 127, 126, 123, 120, 119, 116.8 and 116.2.

Compound **SH6 ((E)-N'-(3-hydroxybenzylidene)-4H-benzo[b][1,4]thiazine-3-carbohydrazide)** yield is (88%) as a pale brown powder; I.R: 3352, 3062, 1666, 1631, 1581, 1311, 1269, 1246, 1157 and 748. ^{1}HNMR (400 MHz, DMSO) δ 12.00 (s, 1H, OH), 10.45 (s, 1H, Ar-NH), 8.65 (s, 1H, Acyc-CH), 7.71 – 7.64 (m, 1H, Ar-CH), 7.33 (s, 1H, Ar-CH), 6.89 (m, 4H, Ar-CH), 6.79 6.72 (m, 2H, Ar-CH), 6.69 (s, 1H, Cyc-NH). ^{13}CNMR: δ 169, 158,149, 135, 130, 128, 127, 126, 125, 123, 122 (for two symmetrical carbons), 119, 116, 113.

Antiproliferative activity evaluation [42]

For academic purposes, the human cancer cell line A504 (small cell lung carcinoma) was obtained. Normal lung cells (NL-20) were cultured in moist conditions at 37°C with 5% CO2 and 95% air. Every two days and 24 hours prior to the conclusion of the experiments, fresh medium was administered. Pre-confluent bulks of cells were passaged using a solution containing 0.05% trypsin and 0.5 mM EDTA. The Biotechnology Research Centre at Al-Nahrain University maintained and examined cell lines that were kept in liquid nitrogen. The MTT assay was used to quantify the finished compounds' antiproliferative efficacy in vitro. At a density of 1x104 cells/well, exponentially budding cells were formed and plated in 96-well plates. After 24 hours of incubation at 37°C under a humidified 5% CO2 to allow cell accessory, the cells in the wells were treated with (SH1-SH6) chemicals at successive concentrations for 48 hours. The cells were not harmed by the DMSO concentration, which was consistently maintained far below 1.25%. Phosphate-buffered saline (PBS; 1.5 mM KH2PO4, 6.5 mM Na2HPO4, 137 mM NaCl, 2.7 mM KCl; pH 7.4) was used to dissolve 3-(4,5-dimethylthizao1–2-y1)-2,5-diphenyltetrazolium bromide (MTT) at a concentration of 5 mg/mL. Each well received 20 µL of this solution added to it. The medium/MTT mixes were separated and the formazan crystals produced by the mitochondrial dehydrogenase activity of energetic cells were dissolved in 100 µL of DMSO per well after the cells were cultivated for four hours at 37°C in a dampened incubator with 5% CO2. A microplate reader (Bio-Rad Instruments) was used to measure the absorbance of the wells at 570 nm. The effects of the chemical on cell viability were computed using cells that had been preserved using DMSO as a control in the ELASIS device, and the IC50 was determined by statistically analyzing the optical density values.

Results and Discussion

According to the Docking Study, erlotinib had a docking value of -9.458 kcal/mol, while the suggested derivatives of SH1, SH2, SH3, SH4, SH5, and SH6 had docking scores of -8.001, -6.086, -7.834, -6.690, -8.729, and -7.842 kcal/mol, respectively. By populating the active site with the majority of interactions of active site protein amino acids, the proposed compounds demonstrated an acceptable active site fitness (Figure 1).

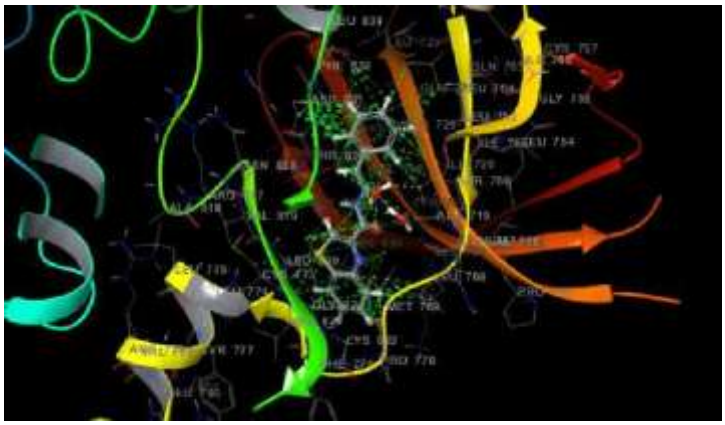

Figure 1. The 3D poses for the interaction of compound SH1 with EGFR-TK isoform (4JHO)

Redocking the co-crystallized ligand into the corresponding receptor's active center and determining the root mean square deviation (RMSD) for the suggested docking algorithm's repeatability and dependability was the first step in validating the molecular modeling technique. The Co-crystallized ligand (erlotinib) was docked separately on EGFR-tyrosine kinase (4HJO), and the RMSD 0.56 Å was less than 2.00 Å, suggesting that the algorithm was verified compared to the crystallographic structure. All derivatives provide an approved receptor fitness by forming a connection with many residues inside the active site, according to a close visual examination of the 2D ligand-receptor interaction. Docking results illustrate that all the docked derivatives (SH1-SH6) have binding energies comparable to that of erlotinib in the proteins' active site, suggesting a potential interaction with the EGFR protein, as it binds through hydrogen bonding in addition to other short contacts that improve the binding. The docking results for all synthesized derivatives (SH1-SH6) revealed a water bridge Hydrogen bond with THR830, and THR766; as well derivatives (SH1, SH2, and SH3) form a hydrogen bond with MET769 via carbonyl moiety; instead of MET769, derivative (SH4) forms a hydrogen bond with PRO770 via OH-moiety, derivatives (SH5 and SH6) form hydrogen bond with MET769 via OH-moiety; additionally, all synthesized derivatives form 9 short contacts with different amino acids [4 hydrophobic interactions with (ALA718, LEU765, LEU820, and VAL702), 4 polar interactions with (ASN818, CYS772, THR765, and THR820), and one glycine interaction with GLY777]. The erlotinib revealed two hydrogen bonds with MET769 and CYS773 and one water bridge hydrogen bond with THR830, and THR766; in addition to the 9 short connects listed above see Table 1 and (Figure 2).

A

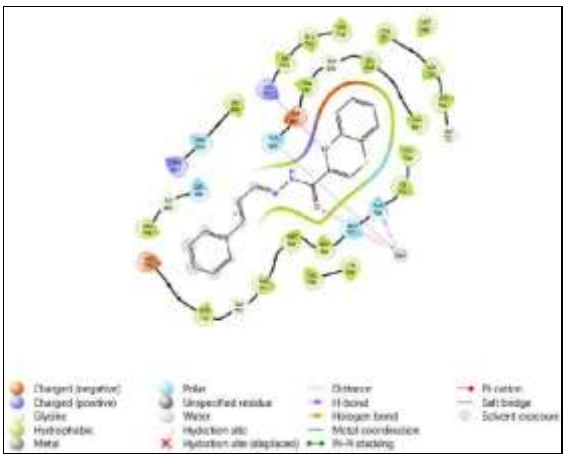

B

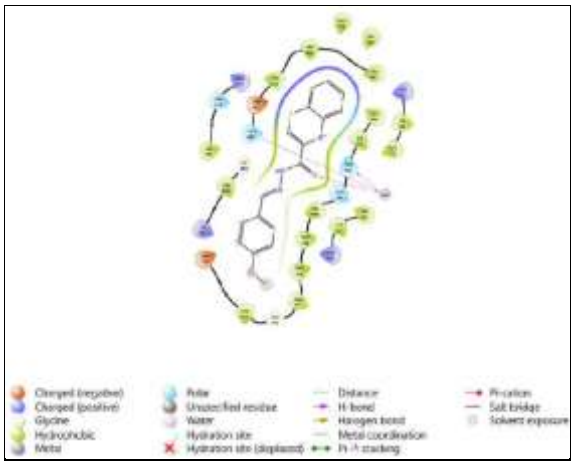

C

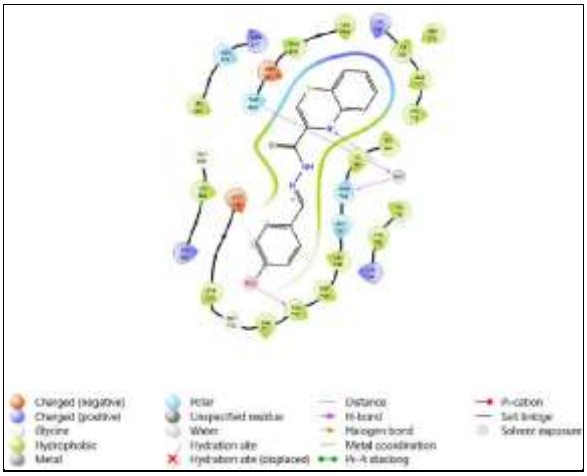

D

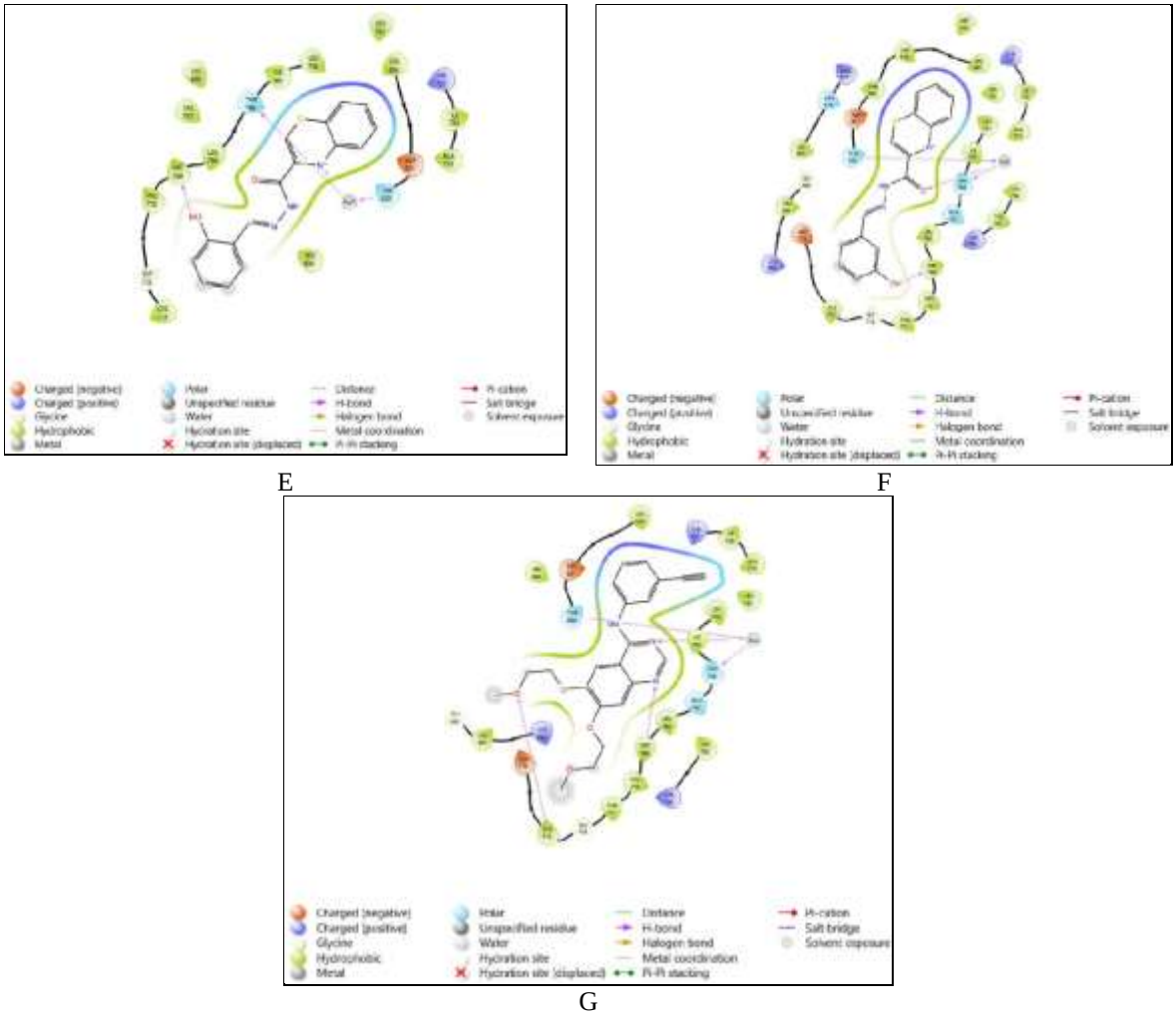

Figure 2. 2D Interaction Diagram of (A) SH1, (B) SH2, (C) SH3, (D) SH4, (E) SH5, (F) SH6, and (G) Erlotinib with EGFR-TK (4HJO).

Table 1. Docking study results include docking score, RMSD, and amino acids of the receptor involved in the connection between ligands and receptor pocket.

Compound	Docking score	RMSD	Amino acids
SH1	-8.403	0.68	MET769, THR830, THR766, ALA718, LEU765, LEU820, VAL702, ASN818, CYS772, THR765, THR820, and GLY777.
SH2	-7.645	0.73	MET769, THR830, THR766, ALA718, LEU765, LEU820, VAL702, ASN818, CYS772, THR765, THR820, and GLY777.
SH3	-7.099	0.70	MET769, THR830, THR766, ALA718, LEU765, LEU820, VAL702, ASN818, CYS772, THR765, THR820, and GLY777.
SH4	-7.461	0.69	PRO770, THR830, THR766, ALA718, LEU765, LEU820, VAL702, ASN818, CYS772, THR765, THR820, and GLY777.
SH5	-8.067	0.67	MET769, THR830, THR766, ALA718, LEU765, LEU820, VAL702, ASN818, CYS772, THR765, THR820, and GLY777.
SH6	-7.627	0.61	MET769, THR830, THR766, ALA718, LEU765, LEU820, VAL702, ASN818, CYS772, THR765, THR820, and GLY777.
Erlotinib	-9.577	0.56	MET769, CYS773, THR830, THR766, ALA718, LEU765, LEU820, VAL702, ASN818, CYS772, THR765, THR820, and GLY777.

ADME-TOX Studies

For the designed molecules to be regarded as drug - like molecules , a number of structural characteristics and attributes must be taken into account. For example, the rule of three and the rule

of five for drugs taken orally are essential strategies for preventing costly late preclinical trials and clinical trial frustration. Acceptable estimated pharmacokinetic characteristics were demonstrated by all synthesized compounds (SH1–SH6). The findings showed a tendency for hydrogen bonding as well as metabolic stability. Furthermore, the compounds do not violate the principles governing drug-like molecules and have calculated oral absorption levels within acceptable ranges (Table 2).

Table 2. The predicted ADMET data for the synthesized compounds

Compound	CNS	#metab	Human Oral Absorption	Percentage of Human Oral Absorption	Rule of five	Rule of three
SH1	0	3	3	100	0	0
SH2	0	3	3	100	0	0
SH3	0	4	3	100	0	0
SH4	-1	4	3	92.38	0	0
SH5	-1	4	3	94.31	0	0
SH6	-1	4	3	93.23	0	0
Erlotinib	-1	6	3	100	0	1

Chemical synthesis

As shown, Scheme. 1 demonstrates the synthesis steps of intermediate compounds A & B. The synthesis involves ester formation starting from p-amino benzenethiol reaction with ethyl 3-bromo-2-oxopropanoate to afford benzothiazine ring with acyclic ester (compound A), which is converted to an amid-containing compound (hydrazide of benzothiazine). Then, new carbohydrazides were prepared by condensing the lately synthesized compound (B) with different cyclic aldehydes giving final compounds (SH1, SH2, SH3, SH4, SH5, and SH6), respectively.

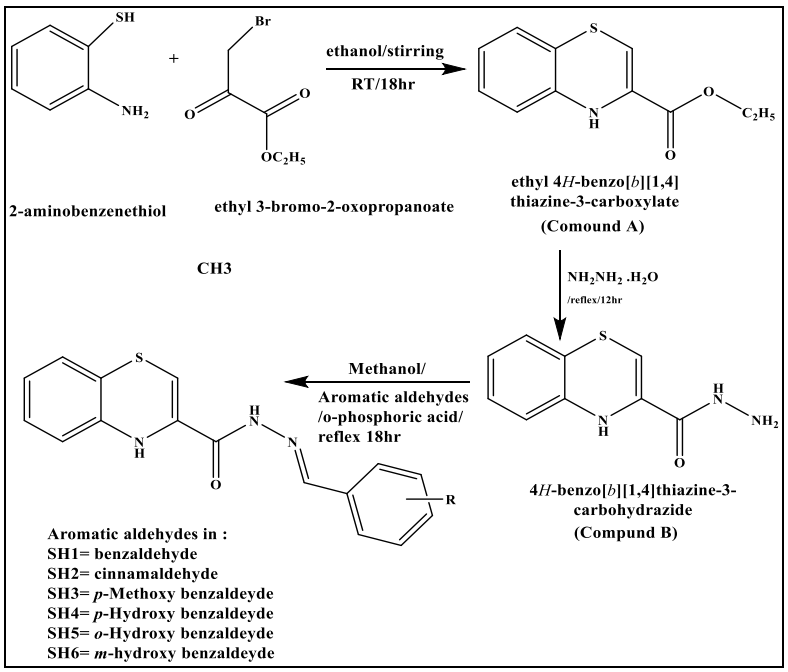

Scheme 1. Synthetic pathway and mechanism of synthesis of new derivatives SH1-SH6

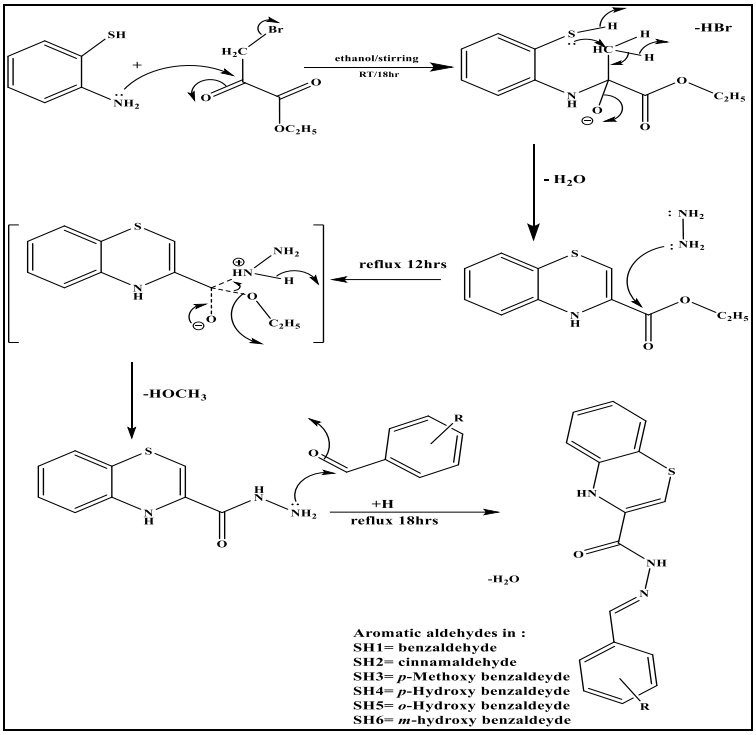

Continued Scheme 1.

Compound studies using thin-layer chromatography were carried out on aluminum foils coated with silica gel. On the aluminum foils, the compound solutions were placed at a spot approximately 2 cm above the lower edge. The polarity of the chemicals determined the chosen mobile phases (Ethyl acetate: hexane). Equipment for measuring the open capillary melting point was used to determine the melting points of synthetic substances. Chemical shifts were expressed in parts per million (δ), and signals were classified as multiple (m), singlet (s), doublet (d), and triplet (t). Compounds were analyzed using thin-layer chromatography, with the polarity of the compounds dictating the preferred mobile phases (ethyl acetate: hexane)) (2.5:7.5). The synthesized compounds were characterized, and their structures were verified by "FTIR, ^{1}HNMR & ^{13}CNMR" spectral analyses.

IR spectra for compounds (A) show characteristic band 1708 ester(C=O), 1674 (C=N), and disappearance of band 1732 (C=O of the acyclic ester of ethyl 3-bromo-2-oxopropanoate). However, compound B shows the disappearance of the ester band and formation of the amide band at (1670) and the appearance of additional bands of NH and NH_2 of hydrazide (3387, 3340 &3244 (NH & NH_2). Also, additional bands at attributed to (Ar-CH stretching) of additional aryl ring and the disappearance of a band of NH_2 of hydrazide in all final compounds (SH1-SH6) with little differentiation among them such as the appearance of 1635 amid (C=O) for SH1, 1658 amid (C=O)for SH2, 1666 amid(C=O) for SH3, 3332 (OH) and 1651 amid(C=O) for SH4, 3352 (OH),1681 amid(C=O) for SH5, 3402 (OH),1655 amid(C=O) for SH6.

^{1}HNMR spectra of the compounds were agreeable with the assigned structures; Compounds (A) show signals at δ= 4.24 – 4.12 (m, 2H, CH_2), 1.22 (t, 3H, CH_3) ppm they will disappear in case of hydrazide compound (B) and instead appeared of 9.35 (s, 1H, Acyc-NH) and 4.38 (s, 2H, NH_2); for SH1 clear additional signals for additional aryl ring and disappearance of the signal of 4.38 (d, 2H, NH_2 of compound B); for compound SH2 we found the appearance of signals at 11.52 (s, 1H, Acyc-NH) and 6.99 – 6.94 (m, 3H, Acyc-CH) ppm; for compound SH3 the appearance of signals at 3.09 (s, 6H, $2CH_3$), 3.65 (s, 6H, 2 OCH_3), 9.49 (s, 1H, NH) ppm was significant; for compounds, SH4, SH5 & SH6 the signal of phenolic OH and acyclic NH groups will be at [11.48(s, 1H, OH), 10.04 (s, 1H, Acyc-NH)], [12.00 (s, 1H, OH), 10.86 (s, 1H, Ar-NH)] &[12.00 (s, 1H, OH), 10.45 (s, 1H, Ar-NH)] respectively.

^{13}C NMR spectra of the compounds were agreeable with the assigned structures; Compound A has specific signals at 161.36 for ester carbonyl carbon, 62.66 for CH_2, and 13.98 for CH_3; these signals will disappear in hydrazide instead of the appearance of signals at 167.45 for amide carbon; for compound SH1apperance of signals at 163.86 for amide carbon,142.74 for imine carbon; for compound SH2 appearance signals of 164.00 for amide carbon and136.28 for imine carbon, for

compound SH3 appearance signals of 159.84 for aryl carbon contact with the methoxy group, 164.07 for amide carbon and149.09 for imine carbon and 55.83 for methoxy carbons; for compound SH4 appearance signals of 157.48 for aryl carbon contact with hydroxide group, 163.94 for amide carbon and141.78 for imine carbon; for compound SH5 appearance signals of 157.86 for aryl carbon contact with hydroxide group, 164.98 for amide carbon and148.98 for imine carbon; for compound SH6 appearance signals of 158.10 for aryl carbon contact with hydroxide group, 169.05 for amide carbon and135.73 for imine carbon.

Anti-proliferative analysis

Survival (%) = [(absorbance of treated cells-absorbance of culture media)/(absorbance of untreated cells-absorbance of culture medium)] x 100 was the formula used to determine cell persistence. The inhibitory concentration (IC) values were determined using a dose-response curve in a triplicate experiment. The concentration in "µM" prepared in a dilution series concentration as (100, 50, 25, 12.5, 6.25, and 3.125 µM) needed to inhibit cell growth by 50% when compared to a control is known as the "IC50." monoclonal (Erlotinib) as a reference. From the rectilinear section of the curve, IC50 values were obtained by determining the agent's concentration that reduced absorbance in pickled cells by 50% when compared to control cells. The estimate is derived from three independent experiments with a minimum of six microcultures per concentration level.

As will noted in Figures. (1 to 6), and Tables 3 the inhibition % and inhibitory concentration (IC50) of all synthesized compounds (SH1-SH6) showed good results of inhibition% (82.3, 88.2, 70.5, 82.3, 82.3, and 94.1); and IC50 (10.24, 5.47, 19.98, 4.18, 13.13, and 3.88) µM for finished products (SH1-SH6) respectively; compared with the inhibition % (94.7%) and IC50 (3.86µM) for reference approved drug (erlotinib); the most promise derivative was SH6 possess inhibition% (94.1%) and IC50 (3.88µM) and lesser one was derivative SH3 possess inhibition%(70.5%) and IC50(19.986µM) that's maybe corresponding to SAR of these derivatives and the tyrosine kinase receptor were they must act as anti-proliferative against lung cancer cell line.

Structure-activity relationships (SAR)

Useful information regarding the structure-activity relationships (SAR) of the newly synthesized derivatives of N'-benzylidene-4H-benzo[b][1,4]thiazine-3-carbohydrazide as Schiff bases (SH1-SH6), as potential EGFR-TK inhibitors, can be highlighted by comparing their structure to erlotinib, specifically those moieties on the reference compounds that make them successful cytotoxic medications. All synthesized derivatives are composed of the same structural skeletons of the hydrophobic center (benzothiazine ring), linker (amide group conjugated to Schiff base), terminal hydrophobic moiety (benzene ring), and terminal substitution except in SH1 and SH2; the difference in the activity of synthesized derivatives may be due to the difference in their fitting in receptor pocket; the presence of *m*-Hydroxyl substituted benzene ring give the most anti-proliferative activity (i.e. lower IC50 value) (compound SH6), then *p*- hydroxy benzene ring (compound SH4) then the α-β unsaturated conjugated Schiff base containing compound SH2 that's due to electronic and/or steric hindrance and which lead the connection of this terminal moiety less than other terminals moieties of rest derivatives. All the synthesized compounds have IC50 less than 20 µM, which indicates a good structural skeleton to give good anti-proliferative activity against small cell lung cancer cell lines.

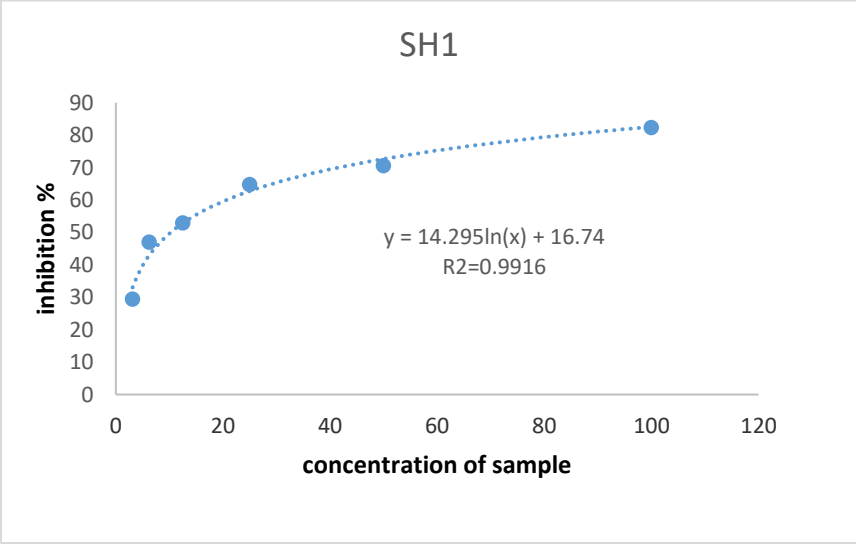

Figure 1: Dose-response curve of SH1

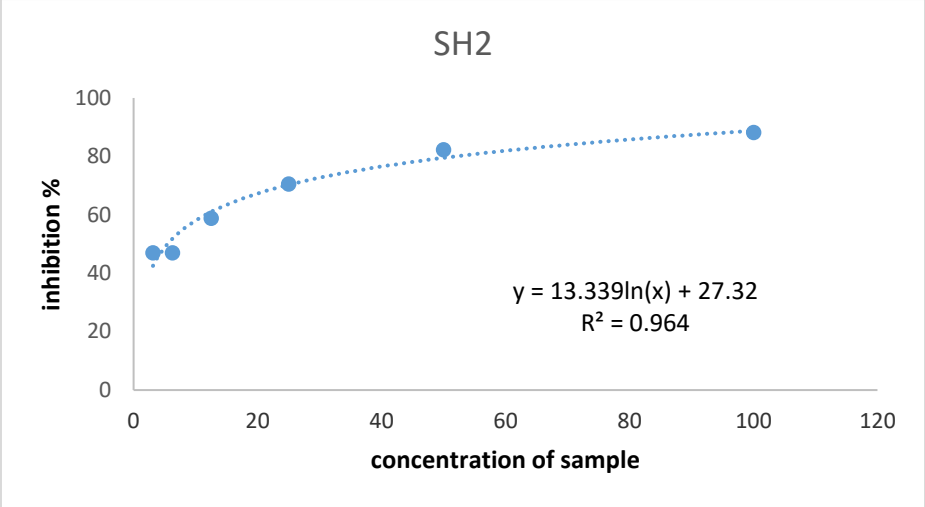

Figure 2. Dose-response curve of SH2

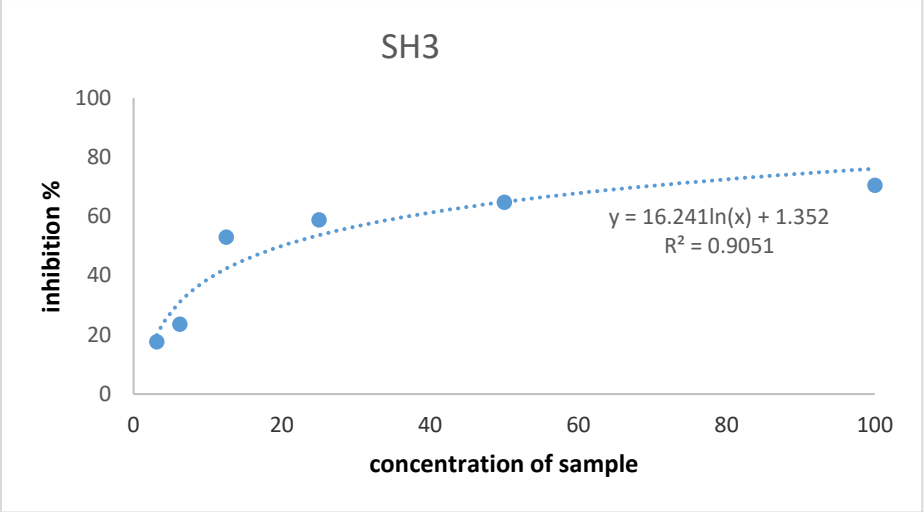

Figure 3. Dose-response curve of SH3

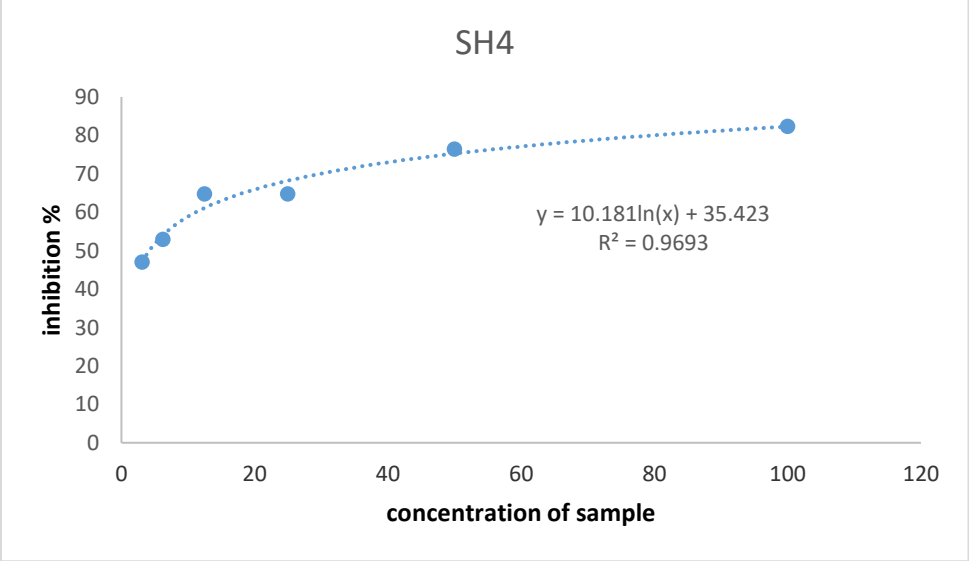

Figure 4. Dose-response curve of SH4

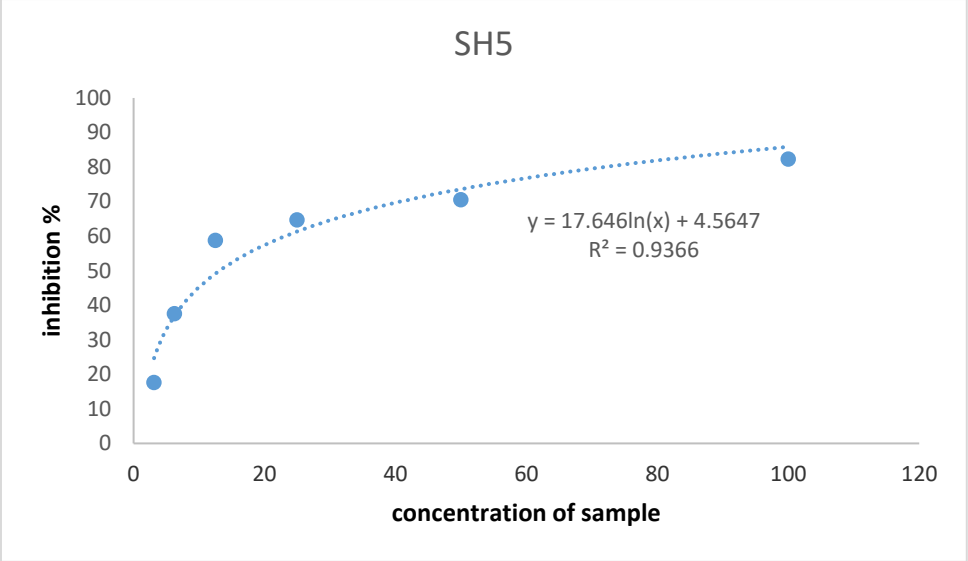

Figure 5. Dose-response curve of SH5

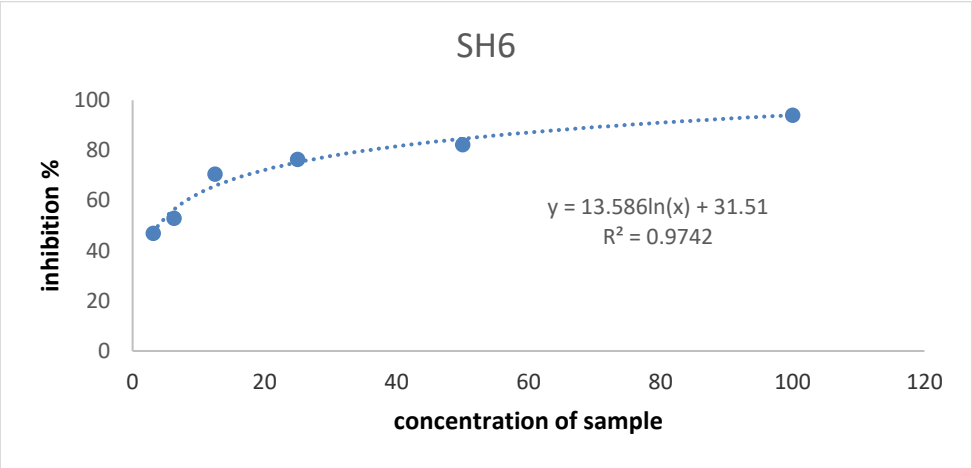

Figure 6. Dose-response curve of SH6

Table 3. Inhibition% and IC50 of Erlotinib and synthetic derivatives SH1-SH6

Compound	Inhibition %	IC50 µM
SH1	82.3	10.24
SH2	88.2	5.47
SH3	70.5	19.98
SH4	82.3	4.18
SH5	82.3	13.13
SH6	94.1	3.88
Erlotinib	94.7	3.86

Conclusion

A novel Schiff bases group containing derivatives was installed to build potential EGFR-TK inhibitors. Using the licensed Glide software, molecular docking tests were conducted to examine the Schiff bases virtually. Although the final compounds had a lower docking score and were practically attached to EGFR-TK, they are still linked to protein amino acids by various interactions, including hydrogen bonds, which have a recognized fitness level. The virtual ADMET experiments revealed that the final drugs had acceptable pharmacokinetic characteristics. Excellent mild organic synthesis techniques were used to effectively synthesize the specified

compounds with acceptable yields. FTIR, ^{1}HNMR, and ^{13}CNMR spectroscopy were used to characterize each of the intermediates and end products. According to the antiproliferative activity investigation, the synthesized compounds showed a promising preliminary inhibition of cancer cells that is similar to that of erlotinib, a tyrosine kinase inhibitor that is employed in clinical settings. With an inhibition percentage of 94.1% and the lowest IC50 (3.88μM) against the A-504 lung cancer cell line, compound SH6 demonstrated the highest cytotoxicity by forming a strong hydrogen bond with MET769 amino acid of the receptor via m-hydroxyl moiety at terminal benzene ring.

Acknowledgment

The University of Baghdad's College of Pharmacy's Pharmaceutical Chemistry Department is duly acknowledged by the writers. The writers truly value evidence. Thank you to Dr. Hayder Al-Hasani, dean of the University of Al-Nahrain's College of Pharmacy, for your assistance in evaluating the antiproliferative potential of the compounds that were developed.

Conflicts of Interest

There isn't any conflict of interest with your manuscript being published.

Funding

The research has not received financial support from an Institution.

Ethics Statements

As per the research integrity regulations in our nation, ethical committee permission is not required for this study.

Author Contribution

The authors confirm their contribution to the paper as follows: study conception and design: Haider J. Al-Karagully and Mohammed Kamil Hadi; data collection: Haider J. Al-Karagully and Mohammed Kamil Hadi; analysis and interpretation of results: Haider J. Al-Karagully and Mohammed Kamil Hadi; draft manuscript preparation: Haider J. Al-Karagully, Mohammed Kamil Hadi. All authors reviewed the results and approved the final version of the manuscript.

References

1. WHO-Cancer. 2022. Available online: https://www.who.int/news-room/fact-sheets/detail/cancer (accessed on 20 December 2022).

2. Alsaad H, Kubba A, Tahtamouni LH, Hamzah AH; Synthesis, docking study, and structure-activity relationship of novel anti-tumor 1, 2, 4 triazole derivatives incorporating 2-(2, 3-dimethyl aminobenzoic acid) moiety. Pharmacia. 2022; 69(2): 415.

3. Roskoski, R. A historical overview of protein kinases and their targeted small molecule inhibitors. Pharmacol. Res. 2015; 100: 1–23.

4. Jampilek, J.; Kralova, K. Insights into lipid-based delivery nanosystems of protein-tyrosine kinase inhibitors for cancer therapy. Pharmaceutics. 2022; 14: 2706.

5. Pottier, C.; Fresnais, M.; Gilon, M.; Jerusalem, G.; Longuespee, R.; Sounni, N.E. Tyrosine kinase inhibitors in cancer: Breakthrough and challenges of targeted therapy. Cancers. 2020; 12:731.

6. Zahavi, D.; Weiner, L. Monoclonal antibodies in cancer therapy. Antibodies. 2020; 9: 34.

7. Jin, S.; Sun, Y.; Liang, X.; Gu, X.; Ning, J.; Xu, Y.; Chen, S.; Pan, L. Emerging new therapeutic antibody derivatives for cancer treatment. Sig. Transduct. Target Ther. 2022; 7: 39.

8. Mohammed Kamil Hadi, Nedaa A. Hameed A. Rahim, Ahmed T. Sulaiman, Rusul Mohammed Hasan Ali. Synthesis, Characterization and Preliminary Antimicrobial Evaluation of New Schiff Bases and Aminothiadiazole Derivatives of N- Substituted Phthalimide. Research J. Pharm. and Tech. 2022; 15(9): (3861)

9. Jampilek, J.; Kralova, K. Anticancer applications of essential oils formulated into lipid-based delivery nanosystems. Pharmaceutics. 2022; 14: 2681.

10. Yang, T.; Zhai, J.; Hu, D.; Yang, R.; Wang, G.; Li, Y.; Liang, G. "Targeting design" of nanoparticles in tumor therapy. Pharmaceutics. 2022; 14: 1919.

11. Shams S. Abdulraheem, Mohammed K. Hadi. Synthesis and Characterization of New Coumarin Derivatives as Possible Antimicrobial Agents. IJDDT. 2021; 11(4): 1484.

12. Fayed, E.A.; Eissa, S.I.; Bayoumi, A.H.; Gohar, N.A.; Mehany, A.B.M.; Ammar, Y.A. Design, synthesis, cytotoxicity and molecular modeling studies of some novel fluorinated pyrazole-based heterocycles as anticancer and apoptosis-inducing agents. Mol. Divers. 2019; 23: 165–181.

13. Vinsova, J.; Cermakova, K.; Tomeckova, A.; Ceckova, M.; Jampilek, J.; Cermak, P.; Kunes, J.; Dolezal, M.; Staud, F. Synthesis and antimicrobial evaluation of new 2-substituted 5,7-di-tert-butylbenzoxazoles. Bioorg. Med. Chem. 2006; 14: 5850–5865.

14. Imramovsky, A.; Pejchal, V.; Stepankova, S.; Vorcakova, K.; Jampilek, J.; Vanco, J.; Simunek, P.; Kralovec, K.; Bruckova, L.; Mandikova, J.; et al. Synthesis and in vitro evaluation of new derivatives of 2-substituted-6-fluorobenzo[d]thiazoles as cholinesterase inhibitors. Bioorg. Med. Chem. 2013; 21: 1735–1748.

15. Taylor, A.P.; Robinson, R.P.; Fobian, Y.M.; Blakemore, D.C.; Jones, L.H.; Fadeyi, O. Modern advances in heterocyclic chemistry in drug discovery. Org. Biomol. Chem. 2016; 14: 6611–6637.

16. Drug Discovery World: The Importance of Heterocyclic Compounds in Anti-Cancer Drug Design. Available online: https://www.ddw-online.com/the-importance-of-heterocyclic-compounds-in-anti-cancer-drug-design-1106-201708/ (accessed on 10 February 2023).

17. Lang, D.K.; Kaur, R.; Arora, R.; Saini, B.; Arora, S. Nitrogen-containing heterocycles as anticancer agents: An overview. Anticancer Agents Med. Chem. 2020; 20: 2150–2168.

18. Amewu, R.K.; Sakyi, P.O.; Osei-Safo, D.; Addae-Mensah, I. Synthetic and naturally occurring heterocyclic anticancer compounds with multiple biological targets. Molecules. 2021; 26: 7134.

19. Kasim S. Hmood, Ammar A. Razzak Mahmood Kubba. Synthesis, Docking Study And In Vitro Anticancer Evaluation Of New Derivatives Of 2-(1-(2-Flouro-[1,1- Biphenyl]-4-Yl)Ethyl)-6-(Substituted Phenyl) Imidazole[2,1-B][1,3,4]Thiadiazole Derived From Flurbiprofen, Sys Rev Pharm. 2021;12(2):184

20. Halah A. Sahib, Mohammed K. Hadi, Maadh Qusay Abdulkadir. Synthesis, and Antimicrobial Evaluation of New Hydrazone Derivatives of (2,4-dinitrophenyl) hydrazine. Research J. Pharm. and Tech. 2022; 15(4): 1743.

21. Pratap, U.R.; Jawale, D.V.; Londhe, B.S.; Mane, R.A. Baker's yeast catalyzed synthesis of 1,4-benzothiazines, performed under Ultrasonication. J. Mol. Catal. B: Enzym. 2011; 68: 94-97.

22. Gupta, R. R.; Jain, M.; Rathore R.S.; Gupta, A. Synthetic and spectral investigation of fluorinated phenothiazines and 4-H-l,4-benzothiazines as potent anticancer agents, J. Fluorine Chem. 1993; 62: 191-200.

23. King, D.J.; Wager, E. Haematological safety of antipsychotic drugs. J. Psychopharmacol. 1998; 12(3): 283-288.

24. Cecchetti, V.; Calderone, V.; Tabarrini, O.; Sabatini, S.; Filipponi, E.; Testai, L.; Spogli, R.; Martinotti, E.; Fravolini, A. Highly potent 1, 4-benzothiazine derivatives as KATP-channel openers. J. Med. Chem. 2003; 46: 3670-3679.

25. Deshmukh, M.B.; Mulik, A.R.; Desai, S.D. Synthesis of some new 2-methyl-1,4-benzothiazin-3-(1H)-one derivatives as potential vasodilator. Eur. J. Chem. 2004; 1(4): 206-210.

26. Rathore, B.S.; Kumar, M. Synthesis of 7-chloro-5-trifluoromethyl/ 7-fluoro/7-trifluoromethyl-4H-1, 4-benzothiazines as antimicrobial agents. Bioorg. Med. Chem. 2006; 14: 5678-5682.

27. Wurood S. Ahmed, Ammar A. Razzak Mahmood, and Redha I. Synthesis and Evaluation of Antimicrobial Activity of New Imides and Schiff Bases Derived from Ethyl-4-Amino Benzoate, Orient. J. Chem. 2022;34(5): 2478.

28. Bray, F.; Ferlay, J.; Soerjomataram, I.; Siegel, R.L.; Torre, L.A.; Jemal, A. Global cancer statistics 2018: GLOBOCAN estimates of incidence and mortality worldwide for 36 cancers in 185 countries. CA Cancer J. Clin. 2018; 68(6): 394-424.

29. Inamura, K. Lung cancer: Understanding its molecular pathology and the 2015 WHO classification. Front. Oncol. 2017; 7: 193.

30. Han, Y.; Li, H. miRNAs as biomarkers and for the early detection of non-small cell lung cancer (NSCLC). J. Thorac. Dis. 2018; 10(5): 3119-3131.

31. Scagliotti, G.; Stahel, R.A.; Rosell, R.; Thatcher, N.; Soria, J.C. ALK translocation and crizotinib in non-small cell lung cancer: An evolving paradigm in oncology drug development. Eur. J. Cancer. 2012; 48(7): 961-973.

32. Sequist, L.V.; Bell, D.W.; Lynch, T.J.; Haber, D.A. Molecular predictors of response to epidermal growth factor receptor antagonists in non-small-cell lung cancer. J. Clin. Oncol. 2007; 25(5): 587-595.

33. Woodman, C. Applications and strategies in nanodiagnosis and nanotherapy in lung cancer. In: Seminars in cancer biology; Elsevier, 2021.

34. Jin H. Park, Yingting Liu, Mark A. Lemmon and Ravi Radhakrishnan. Erlotinib binds both inactive and active conformations of the EGFR tyrosine kinase domain, Biochem. J. 2012; 448: 417–423.

35. Saad, AM, and Al-Hamashi, AA. Molecular Docking, ADMET Study, Synthesis, Characterization, and Preliminary Antiproliferative Activity of Potential Histone Deacetylase Inhibitors with Isoxazole as New Zinc Binding Group. Iraqi J Pharm Sci, 2023; 32(Suppl.):188-203.

36. Péter Kisszékelyi, Tibor Peňaška, Klára Stankovianska, Mária Mečiarová and Radovan Šebesta. Derivatives of benzo-1,4-thiazine-3-carboxylic acid and the corresponding amino acid conjugates, Beilstein J. Org. Chem. 2022; 18: 1197.

37. Al-Karagully HJ, and Hadi MK. Synthesis, Characterization, And Anti-Proliferative Activity Study of Novel Derivatives Of N'-(4h-Benzo[B] [1,4] Thiazine-3 Carbonyl) Benzene Sulfone-Hydrazides Against Lung and Breast

Cancer Cell Line. Afr. J. Biomed. Res. December 2024; 27(4s): 10219 -10233.

38. Kamms ZD, Hadi MK. Synthesis, Characterization and Preliminary Antimicrobial and Anti-inflammatory Evaluation of New Ibuprofen Hydrazide Derivatives. International Journal of Drug Delivery Technology. 2023;13(1):376-38.

39. Al-Karagully HJ, and Hadi MK. Molecular docking, ADMET, synthesis and anti-proliferative of novel derivatives of benzothiazine against lung cancer cell line. J Adv Pharm Educ Res. 2025;15(1): 67-75.

40. Omeed M. Hassan, Ammar A. Razzak Mahmood, Ali H. Hamzah, and Lubna H. Tahtamouni. Design, Synthesis, and Molecular Docking Studies of 5- Bromoindole-2-Carboxylic Acid Hydrazone Derivatives: In Vitro Anticancer and VEGFR-2 Inhibitory Effects, Chemistry Select. 2022; 7(9): 3726.

41. Hamdoon YS, and Hadi MK. Molecular docking, ADMET, synthesis and evaluation of new indomethacin hydrazide derivatives as antibacterial agents. Pharmacia. 2024; 71: 1–10

42. Shamsuzzaman, Ayaz Mahmood Dar, Hena Khanam, Manzoor Ahmad Gatoo, Anticancer and antimicrobial evaluation of newly synthesized steroidal 5,6 fused benzothiazines. Arabian Journal of Chemistry. 2014; 7(4): 461-468.

الرسو الجزيئي ، دراسة الحركة الدوائية ، تخليق ، تشخيص ودراسة النشاط المضاد للتكاثر لمشتقات قاعدة شيف الجديدة لـ (ان)-بنزليدين-٤أج-بنزو [ب][١،٤]ثيازين-٣-كربوهيدرازيد ضد خط خلايا سرطان الرئة.

حيدر جبار القرغولي*[١] و محمد كامل هادي[٢]

[١]وزارة الصحة، المركز الوطني للرقابة والبحوث الدوائية، بغداد، العراق.

[٢]قسم الكيمياء الصيدلانية، كلية الصيدلة، جامعة بغداد، بغداد، العراق.

الخلاصة

يعد مستقبل عامل نمو البشرة التيروزين كيناز (EGFR-TK) هدفًا جينيًا مثيرًا للاهتمام للغاية للعلاج الدوائي. يتم التعبير عن EGFR-TK بشكل مفرط في العديد من الأمراض، بما في ذلك السرطان. في هذا العمل، قمنا بتصميم مثبطات EGFR-TK جديدة تحتوي على نفس المكون من إرلوتينيب (دواء مضاد للسرطان معتمد) مع رابط أطول وجزء النافر للماء المعوض باستخدام برنامج التصميم الدوائي من شرودنكر. تم تحسين الرابط من خلال تجربة العديد من بقايا الأميد وقاعدة شيف. تم تقييم التثبيط المحتمل على EGFR-TK للمنتجات المصممة بشكل مثالي باستخدام برنامج نمذجة شرودنكر المرخص. أظهرت النتائج أن الشق الكاره للماء لاستبدال الهيدروكسيل له تفاعل محتمل مع الموقع النشط EGFR-TK مع ملاءمة مقبولة. تم إجراء دراسة ADMET للتنبؤ بالخصائص الدوائية للمركبات النهائية. أظهرت المركبات النهائية خصائص شبيهة بالدواء مقدرة بشكل جيد. تم تصنيع وتنقية المركبات الوسيطة والنهائية بنجاح باستخدام إعادة البلورة. تم تشخيص التركيب الكيميائي للمركبات الوسيطة والنهائية بواسطة التحليل الطيفي بالاشعة تحت الحمراء FTIR، والتحليل الطيفي بالرنين المغناطيسي النووي للبروتون ونظير الكاربون ١٣(HNMR[١]، وCNMR[١٣]) . باستخدام تقنية MTT ، كشفت جميع المركبات المصنعة (SH1-SH6) عن نشاط مضاد للأورام مشجع في خطوط خلايا سرطان الرئة A504 مع IC50 بقيمة ١٠,٢٤ ميكرومول، ٥,٤٧ ميكرومول، ١٩,٩٨ ميكرومول، ٤,١٨ ميكرومول، ١٣,١٣ ميكرومول، و ٣,٨٨ ميكرومول على التوالي، ونسبة تثبيط ٨٢,٣٪، ٨٨,٢ %، ٧٠,٥٪، ٨٢,٣٪، ٨٢,٣٪، و٩٤,١٪ على التوالي، وهو ما يشبه إرلوتينيب IC50 الذي يبلغ ٣,٨٦ ميكرومتر ونسبة التثبيط ٩٤,٧٪. كان المركب SH6 هو المركب الواعد (IC50=3.88µM ونسبة التثبيط=٩٤,١٪)، مقارنة مع erlotinib، وهو عقار مرجعي معتمد مضاد للسرطان.

الكلمات المفتاحية: الحركية الدوائية، مكافحة التكاثر، البنزوثيازين، إرلوتينيب، سرطان الرئة، الرسو الجزيئي، قواعد شيف.